Gene 498 (2012) 147–154

Contents lists available at SciVerse ScienceDirect

Gene

journal homepage: www.elsevier.com/locate/gene

Cloning, localization and differential expression of the *Trypanosoma cruzi Tc*OGNT-2 glycosyl transferase

María Laura Chiribao [a,b], María Gabriela Libisch [a], Eduardo Osinaga [c], Adriana Parodi-Talice [a,d], Carlos Robello [a,b,*]

[a] *Unidad de Biología Molecular, Institut Pasteur de Montevideo, Uruguay*
[b] *Departamento de Bioquímica, Facultad de Medicina, Universidad de la República, Uruguay*
[c] *Departamento de Inmunobiología, Facultad de Medicina, Universidad de la República, Uruguay*
[d] *Sección Genética, Facultad de Ciencias, Universidad de la República, Montevideo, Uruguay*

ARTICLE INFO

Article history:
Accepted 14 February 2012
Available online 25 February 2012

Keywords:
Chagas disease
Glycosyl-transferase
Differential expression
O-glycosylation
Infectivity

ABSTRACT

The surface of *Trypanosoma cruzi* is covered by a dense glycocalix which is characteristic of each stage of the life cycle. Its composition and complexity depend mainly on mucin-like proteins. A remarkable feature of *O*-glycan biosynthesis in trypanosomes is that it initiates with the addition of a GlcNAc instead of the GalNAc residue that is commonly used in vertebrate mucins. The fact that the interplay between *trans*-sialidase and mucin is crucial for pathogenesis, and both families have stage-specific members is also remarkable. Recently the enzyme that transfers the first GlcNAc from UDP-GlcNAc to a serine or threonine residue was kinetically characterized. The relevance of this enzyme is evidenced by its role as catalyzer of the first step in *O*-glycosylation. In this paper we describe how this gene is expressed differentially along the life cycle with a pattern that is very similar to that of *trans*-sialidases. Its localization was determined, showing that the protein predicted to be in the Golgi apparatus is also present in reservosomes. Finally our results indicate that this enzyme, when overexpressed, enhances *T. cruzi* infectivity.

1. Introduction

Mucins are cell surface or secreted glycoproteins with large numbers of clustered *O*-glycans (Jensen et al., 2010). The surface of *Trypanosoma cruzi* is covered with mucins which are anchored to the membrane by glycosylphosphatidylinositol (GPI) and constitute major surface components in these parasites (Acosta-Serrano et al., 2001). Mucins are strongly implicated in *T. cruzi* biology, contributing to host invasion, parasite protection, and also to the establishment of persistent infections (Buscaglia et al., 2006). The mucin-gene repertoire in *T. cruzi* shows high complexity; hundreds of genes have been identified (Di Noia et al., 1998) and arranged into two main families on the basis of sequence homology (Freitas-Junior et al., 1998) (i) the *Tc*SMUG (*T. cruzi* small mucin gene) family, a homogeneous family of 70–80 genes that encode for mucins that are expressed in the insect stage, and (ii) the *Tc*MUC family which comprises 500–700 genes that encode for mucins present in the mammal-dwelling stages. The transition from insect-dwelling to mammal-dwelling stages leads to the use of different, non-overlapping sets of mucin genes, switching from a mucin coat of a rather homogeneous polypeptide composition to a highly heterogeneous one (Buscaglia et al., 2006). The genome of *T. cruzi* revealed another large gene family (corresponding to approximately 6% of the parasite's diploid genome), encoding mucin-associated surface proteins (MASP) (El-Sayed et al., 2005), which are predominantly expressed in the trypomastigote form (Atwood et al., 2005).

The glycosylation of *T. cruzi* mucins presents some unusual features when compared to its mammalian counterpart (de Lederkremer and Agusti, 2009). Firstly, the biosynthesis of *O*-glycans in *T. cruzi* mucins initiates with the addition of an *N*-acetylglucosamine (GlcNAc) residue linked to serine or threonine residues in the protein backbone, rather than *N*-acetylgalactosamine (GalNAc). Secondly, a proportion of the *O*-linked GlcNAc residues remain unsubstituted, whereas the remainders are further elongated with up to five galactose residues (Acosta-Serrano et al., 2001). Finally, terminal β-galactopyranosyl residues can then be extracellularly decorated with sialic acid. *T. cruzi* incorporates sialic acid in a reaction catalyzed by *trans*-sialidase (TS), a unique parasite enzyme that transfers sialic acid residues from host glycoconjugates to parasite mucins. TS activity enables *T. cruzi* to circumvent its lack of *de novo* synthesis of sialic acid (Previato et al., 1985). It has been demonstrated that sialylation of mucins is crucial for the viability and propagation of these parasites (Pereira-Chioccola et al., 2000).

Abbreviations: GlcNAc, N-acetylglucosamine; *Tc*OGNT-2, *Trypanosoma cruzi O*-GlcNAc-transferase 2; GPI, glycosylphosphatidylinositol; *Tc*MUC, *Trypanosoma cruzi* mucin; TS, *trans*-sialidase; DAPI, 4′,6-diamidino-2-phenylindole.

* Corresponding author at: Unidad de Biología Molecular, Institut Pasteur de Montevideo. Mataojo 2020, CP 11400, Montevideo, Uruguay. Tel.: +598 25220910; fax: +598 25224185.
E-mail address: robello@pasteur.edu.uy (C. Robello).

0378-1119/$ – see front matter © 2012 Elsevier B.V. All rights reserved.
doi:10.1016/j.gene.2012.02.018

Sialylated mucins are involved in many processes, such as protection against proteases (Mortara et al., 1992), recognition and invasion of mammalian host cells (Araguth et al., 1988; Neira et al., 2003; Ruiz Rde et al., 1993; Yoshida et al., 1989, 1990) and immunomodulation (Almeida et al., 1994, 2000). In addition, TS molecules (anchored to the parasite membrane or shed into the bloodstream) can bind to mammalian cell receptors and undermine host defense mechanisms (Chuenkova and Pereira, 1995; Freire-de-Lima et al., 2010; Mucci et al., 2002; Tribulatti et al., 2005).

The biosynthesis of *O*-glycans in mucins in *T. cruzi* initiates with the addition of a GlcNAc residue from UDP-GlcNAc (the activated sugar donor) to serine or threonine residues in the protein by a uridine diphospho-*N*-acetylglucosamine:polypeptide-α-*N*-acetylglucosaminyltransferase (ppGlcNAc-transferase) (Previato et al., 1998). This reaction represents a major difference between *O*-glycosylation in *T. cruzi* and mammals. In mammals the ortholog enzyme is an UDP-GalNAc transferase that transfers N-acetylgalactosamine (GalNAc) from UDP-GalNAc to the peptide (Ten Hagen et al., 2003). This difference may have been originated by the fact that *T. cruzi* is incapable of interconverting UDP-GlcNAc to UDP-GalNAc (Roper and Ferguson, 2003). Recently a *Tc*OGNT-2 gene that encodes a ppGlcNAc-transferase activity was described in *T. cruzi*. Enzymatic analysis showed high levels of UDP-GlcNAc transferase and UDP-GlcNAc hydrolase activities, both specific for UDP-GlcNAc (Heise et al., 2009). The peptide preference and the optimum pH are comparable to the native GlcNAc-transferase activity previously reported in *T. cruzi* microsomal fraction (Previato et al., 1998). The distinctive characteristic of this enzyme, which is not present in the parasite's hosts, suggests that it could be a promising target for chemotherapy. The objective of this work was to analyze *Tc*OGNT-2 through its subcellular localization, expression pattern and its relevance in invasion and infection, under the assumption that its enzymatic activity may be crucial to achieve a fully developed parasite surface with mature mucins, competent for host invasion and parasite protection. Moreover, since this enzyme participates in the initiation of *O*-glycosylation, needed for the subsequent addition of sialic acid by TS, we compared the expression of both enzymes during the invasion process.

2. Materials and methods

2.1. Parasites

Dm28c *T. cruzi* strain was used throughout this work. Epimastigotes were grown in liver infusion tryptose medium (LIT) supplemented with 10% heat inactivated fetal bovine serum (FBS) at 28 °C. Trypomastigotes were collected from supernatants of infected monolayers of Vero cells.

Extracellular amastigotes were obtained by incubating recently released trypomastigotes from infected cells in DMEM medium at 37 °C under 5% CO_2. After 24 h of extracellular incubation the parasite population consisted exclusively of amastigotes.

Metacyclic trypomastigotes were obtained under chemically defined conditions as previously described (Contreras et al., 1985). Metacyclogenesis was triggered through nutritional stress, and epimastigotes undergoing differentiation process were collected at 3, 12 and 24 h after the induced stress.

2.2. Infection assays

Semi confluent Vero cells (70%) were infected with trypomastigotes at a ratio of 5 parasites per cell in 12 well plates with coverslips. Cells were infected for 4 h in DMEM-10% FBS and after infection the cells were washed with PBS and medium was replaced with fresh DMEM-2% FBS. Coverslips were removed at different times post-infection and fixed with ethanol during 5 min. Cells were mounted with ProLong Gold antifade with Dapi (Invitrogen) and the number of infected cells and amastigotes per infected cell were determined by counting the nucleus of Vero cells and the kinetoplast of amastigotes through epifluorescence microscopy.

2.3. DNA, RNA and protein extraction

Whole *T. cruzi* DNA was obtained by phenol-chloroform extraction (Sambrook et al., 1989). RNA was purified from parasites using RNeasy Mini Kit (QIAGEN) and its integrity was analyzed on a Bioanalyzer (Agilent).

For total protein extracts parasites were washed twice in cold PBS and resuspended in lysis buffer (7 M Urea, 2 M Thiourea, 40 mM Tris, 4% CHAPS and 1 mM PMSF) with protease inhibitor cocktail (Roche), under agitation. After centrifugation at 12,000 *g* the supernatant was collected and stored at −80 °C. Proteins were quantified with Bradford reagent (Sigma).

For subcelullar fractionation, 10×10^9 epimastigotes were washed twice in cold PBS, and harvested by centrifugation. The pellet was weighed and twice the weight was added in volume of Silicon carbide (Sigma). The mixture was mechanically disrupted in a mortar and resuspended in 10 mL of sacarose buffer (Tris 25 mM pH 7.6, Sacarose 0.25 M, EDTA 1 mM) and centrifuged at 26 *g* for 3 min. The supernatant, which is the total homogenate (H), was centrifuged at 956 *g* for 10 min and the pellet (nuclear fraction) was resuspended in 1 mL of sacarose buffer. The post nuclear fraction was centrifuged at 5017.6 *g* for 10 min, the pellet (mitochondrial fraction) was also resuspended in 1 mL of sacarose buffer, and the supernatant was finally ultracentrifuged at 80,638 *g* for 1 h obtaining the microsomal fraction (pellet) and the cytosolic fraction (supernatant).

2.4. Cloning, expression analysis and characterization of 3′ and 5′ UTRs of *TcOGNT-2*

The *Tc*OGNT-2 gene was amplified with *Pfu* DNA polymerase (Fermentas) from genomic DNA by polymerase chain reaction (PCR) using the primers *Tc*OGNT-2F: GGTCTAGATCTATGGATAAAAGGAAGC TTGGACG and *Tc*OGNT-2R: CCGAATTCTTATCCAAGTGTTGCCTTTTC, including restriction sites for the *Bgl*II and *Eco*RI enzymes which are underlined.

The fragment was purified and incubated with 0.2 mM dATP and *Taq* DNA polymerase for 20 min at 70 °C and then ligated into the pGEM-T Easy cloning vector (Promega). The plasmid containing *Tc*OGNT-2 was purified by alkaline lysis and fully sequenced.

In order to evaluate *Tc*OGNT-2 mRNA expression in epimastigotes, amastigotes and trypomastigotes, cDNA was produced from total RNA using Superscript II reverse transcriptase (Invitrogen) and an oligo dT as primer. *Tc*OGNT-2 5′ UTR was obtained by PCR amplification with Taq DNA polymerase (Fermentas) using one primer corresponding to the spliced leader (SLTc primer: CGCTATTATTGATACAGTTTCTG) and the specific *Tc*OGNT-2 reverse primer (*Tc*OGNT-2R2): CGGTACCTTAGGGCATTGCGTCGGAAGAACC, *Kpn* I restriction site is underlined. The PCR product was cloned into pGEM-T Easy vector (Promega) and sequenced.

*Tc*OGNT-2 3′ UTRs were obtained by PCR using *Tc*OGNT-2 forward specific primer *Tc*OGNT-2F5 (GTGGAACTTAGTGATGAGTTTGTG) and reverse oligo dT-anchor primer (5′-CCTCTGAAGGTTCACGGATCCACATCTAGA $[T]_{18}$). For hemi-nested PCR the forward primer was *Tc*OGNT-2F2 (5′-CACTTTGGATTGGGGATGTTGCGA). PCR products were cloned in pGEM-T Easy (Promega) and sequenced.

2.5. Protein expression and antibody production

A DNA fragment (408 pb corresponding to residues 51 to 187 in the protein) was PCR amplified using *Tc*OGNT-2 specific forward (GGAGATCTGATGCAGACGGCATTCTTCAG) and reverse (CGGTACCTTAGGGCA

TTGCGTCGGAAGAACC) primers with additional *Bgl*II and *Kpn*I restriction sites respectively. The PCR product was cloned into pGEM-T Easy (Promega), sub-cloned in pQE30 (Qiagen) and expressed in the M15 *E. coli* strain. The expression of the hexahistidine-tag recombinant protein was achieved after induction with 1 mM IPTG during 5 h at 37 °C, and purification through a Ni^{2+} resin column was carried out under denaturing conditions following manufacturer instructions.

Polyclonal antiserum was elicited from New Zealand White rabbits using 200 μg of recombinant *Tc*OGNT2 protein in Freund's Complete Adjuvant (Sigma) for the first immunization. Rabbits were boosted three times with the same amount of protein using Freund's Incomplete Adjuvant (Sigma). Serum was obtained 14 days after the last booster and affinity purified in a Protein A Sepharose column (Sigma) according to manufacturer's recommendations.

2.6. SDS PAGE, Western blot and indirect immunofluorescence

T. cruzi protein extracts (30 μg) were electrophoresed in a 12% polyacrylamide gel (SDS-PAGE) under reducing conditions and visualized by Coomassie staining or electrotransferred to a nitrocellulose membrane (GE Healthcare). Membranes were blocked in 5% skimmed milk in PBS for 16 h at 4 °C or 2 h at 22 °C. After washing with PBS/0.2% Tween 20, membranes were incubated with an appropriate dilution of antibodies for 1 h at room temperature, washed and incubated with peroxidase-conjugated goat anti-rabbit or anti-mouse secondary antibody (Sigma). The signal was developed with chemoluminiscence (ECL, GE Healthcare).

For indirect immunofluorescence (IIF) assays, parasites were washed 3 times with cold PBS and fixed for 20 min at room temperature with 5% paraformaldehyde in PBS and washed again with PBS. After fixation parasites were incubated with 0.1 M glycine and permeabilized in 0.2% Triton ×100 for 10 min at room temperature. One million parasites were allowed to adhere for 30 min to polylysine pre-treated slides. Slides were blocked 2 h at 37 °C with 3% BSA and incubated with polyclonal antibodies (anti-*Tc*OGNT-2 1/200), anti-cytosolic tryparedoxin peroxidase, (c-*Tc*TXNPx, 1/1000) or with anti-SAPA monoclonal antibodies (kind gift from Dr. Oscar Campetella). After washes with PBS-0.1% Tween 20, slides were incubated with ALEXA 488 conjugated goat anti-rabbit (1/1000 for anti-*Tc*OGNT-2 and anti-c-*Tc*TXNPx), or anti-mouse (1/1000 for anti-SAPA) secondary antibody. After 3 washes the slides were mounted with ProLong Gold antifade with DAPI (Invitrogen) and visualized under an epifluorescent Olympus IX 81 microscope coupled to a Hamamatsu Orca-ER camera (Diagnostic Instruments). Visualization of the Golgi complex was achieved with boron-dipyrromethene FL C5 ceramide (Bodipy, Molecular Probes) staining, which was carried out following manufacturer's instructions.

2.7. Real time PCR

*Tc*OGNT-2 mRNA levels were detected by real time PCR. A 400 pb fragment was amplified from epimastigote, trypomastigote or amastigote cDNA with the forward primer Ac*Tc*OGNT-2F (GGAGATCTGATGCAGACGGCATTCTTCAG) and reverse primer Ac*Tc*OGNT-2R (CGGTACCTTAGGGCATTGCGTCGGAAGAACC). The GAPDH gene was used as a reference for normalization. The total volume reaction was 10 μL:1 μL of each primer (1 μM), 5 μL of SYBER MIX (Quantimix Easy Syg Kit, Biotools), 1 μL of cDNA and 2 μL of water. The amplification was performed in a Corbett Research RG-6000 termocycler with the following parameters: 95 °C for 10 min, 40 cycles of 95 °C for 15 s, 58 °C for 30 s and 72 °C for 30 s. The PCR for each cDNA was performed in duplicate. The amount of *Tc*OGNT-2, relative to the reference GAPDH gene, was calculated using the comparative Ct method (ΔΔCt method), and expressed as an n-fold variation of *Tc*OGNT-2 levels in amastigotes and epimastigotes samples when compared to the trypomastigotes sample. PCR specificity was checked by melting curves.

2.8. Production of T. cruzi cell lines over-expressing TcOGNT-2

The entire *Tc*OGNT-2 gene was amplified from genomic DNA and cloned into pGEM-T Easy (Promega). After complete sequencing, the fragment was excised with *Bam*HI and *Eco*RI enzymes and ligated into the trypanosomal expression vector pTEX (Kelly et al., 1992), generating the pTEX-*Tc*OGNT-2 construction.

For transfection, 5×10^7 epimastigotes were resuspended in 450 μL of HES Buffer (21 mM HEPES, 137 mM NaCl, 5 mM KCl, 7 mM Na_2HPO_4, 6 mM glucose, pH 7.4) and electroporated with 50 μg of pTEX or pTEX-*Tc*OGNT-2 DNA in a BTX ElectroCell Manipulator 600 using two pulses at 450 V, 1300 μF and 13 Ω in 4 mm cuvettes. Transfected parasites were grown in the presence of continually increasing G418 (GIBCO) concentrations up to 1 mg/mL. Overexpression was confirmed by Western blot and real time PCR.

2.9. Statistical analysis

Real time PCR results were tested for significance by a Pair Wise Fixed Reallocation Randomization Test using the REST (Relative Expression Software Tool) program. The Unpaired Student *t* Test was used to calculate a significant difference in the infection assay between pTEX transfected parasites and parasites over-expressing pTEX-*Tc*OGNT-2. Differences were considered significant when $p<0.05$. The analysis was carried out using GraphPad Prism, version 3.0 (GraphPad Software, San Diego, CA).

3. Results

3.1. TcOGNT-2 is located in the Golgi apparatus and reservosomes

In order to study the localization of *Tc*OGNT-2, we carried out subcellular fractionation by differential centrifugation. Each fraction was analyzed by Western blot using anti-*Tc*OGNT-2 antiserum. As shown in Fig. 1A, *Tc*OGNT-2 was highly enriched in the microsomal fraction obtained after ultracentrifugation of the post-mitochondrial fraction. The subcellular localization of *Tc*OGNT-2 was also analyzed by indirect immunofluorescence. Fig. 1B shows that the labeling of *Tc*OGNT-2 is clearly localized in two main regions in the parasite: a weaker stain in the anterior region of the epimastigote form, next to the kinetoplast, and a stronger and granular labeling in the posterior region. Since this distribution resembles the location of the Golgi apparatus and reservosomes respectively (Cunha-e-Silva et al., 2006), we compared *Tc*OGNT-2 staining with the Golgi marker Bodipy FL5 ceramide and with an anti cruzipain antibody which recognizes a protein described as a reservosome marker (Sant'Anna et al., 2008a). Labeling of *Tc*OGNT-2 showed the same distribution as both ceramide and cruzipain, thus strongly suggesting that *Tc*OGNT-2 is located in the Golgi apparatus as well as in reservosomes.

3.2. TcOGNT2 is differentially expressed along the life cycle of Trypanosoma cruzi

The expression of *Tc*OGNT-2 during the life cycle of *T. cruzi* was analyzed by Western blot using total extracts from the different stages of the parasite. The purified antibody obtained against *Tc*OGNT-2 recognized a band of 59 kDa, in accordance with the expected molecular weight of this protein. *Tc*OGNT-2 was found to be expressed in epimastigotes, cell derived trypomastigotes and metacyclic trypomastigotes. Since a number of changes occur in mucin patterns during metacyclogenesis (Acosta et al., 1994), we analyzed this process more in detail. We observed that *Tc*OGNT-2 levels increased during the metacyclogenesis process, as shown in Fig. 2A:

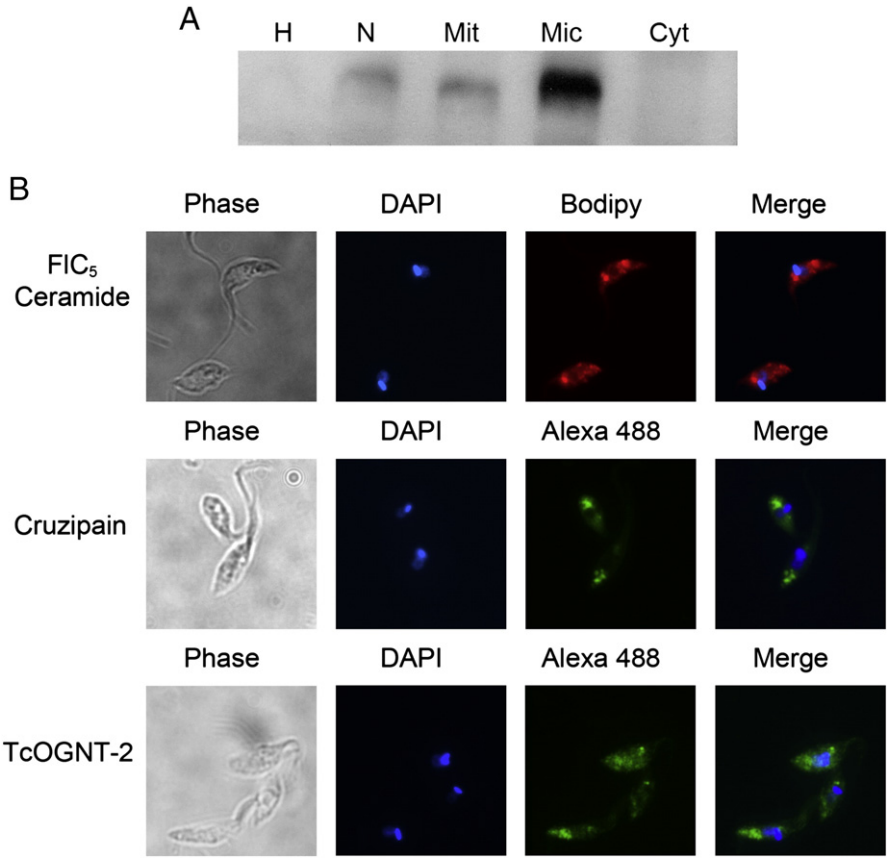

Fig. 1. Expression and localization of *Tc*OGNT-2 in epimastigotes: A: Western blot with 10 μg of total protein extract of each subcellular fraction. H (total homogenate), N (nuclear fraction), Mit (mitochondria), Mic (microsomal fraction) and Cyt (cytoplasmic fraction) probed with anti *Tc*OGNT-2 antiserum.B: Permeabilized epimastigotes were stained with DAPI and incubated with anti *Tc*OGNT-2 purified antibodies (diluted 1/200) or with anti cruzipain antibody (1/200) as a reservosome marker. Parasites were also stained with Bodipy FL 5 ceramide for Golgi complex visualization.

the differentiation from epimastigotes to metacyclic trypomastigotes was associated with an increased expression of *Tc*OGNT-2, that showed its peak in trypomastigotes. Remarkably, *Tc*OGNT-2 protein expression was not detected at all in extracts from amastigotes, indicating that the protein is differentially regulated along the life cycle of the parasite. Since amastigotes represent the predominant stage during the intracellular phase of the *T. cruzi* life cycle, we studied the expression of *Tc*OGNT-2 by IIF, paying particular attention to the infection process, i.e. the early and late infection. Consistent with the western blot results, the enzyme was found to be expressed both in epimastigotes and cell derived trypomastigotes and, in contrast, the protein displayed almost undetectable levels in axenic amastigotes (Fig. 2B). In the same direction, we observed that in the axenic cultures some parasites which were differentiating to trypomastigotes (evidenced as slender forms), showed a significant change in protein expression (Fig. 2B), suggesting a specific upregulation for this enzyme in the passage from amastigotes to trypomastigotes.

3.3. The TcOGNT-2 expression, as that of trans-sialidase, is "switched off" during the early infection process

From the above results, and taking into account that this protein participates in the initiation of mucin-type *O*-glycosylation in *T. cruzi*, we hypothesized that *Tc*OGNT-2 differential expression along the life cycle could be related to the changes in mucin profiles produced during invasion. If this were the case, a coordinated expression with *trans*-sialidase would ensure at least a change in the *O*-glycosylation profiles of mucins in these parasites. Previous studies on TS expression during *T. cruzi* infection showed that amastigotes lose the TS from their surface as soon as they enter the host cell (Frevert et al., 1992). In order to compare the expression of both proteins, infected Vero cells were fixed at different post infection times (0, 24, 48, 72, 96 and 120 h) and then parasites were stained with DAPI and incubated either with anti *Tc*OGNT-2 antiserum or an anti SAPA antibody which recognizes SAPA repeats present in *trans*-sialidases (Buscaglia et al., 1998) Fig. 3 shows that TS begins to be faintly detected after 48 h, being the parasites clearly positive for TS expression at 96 h post infection. On the other hand, labeling of infected cells with anti *Tc*OGNT-2 antibody was detectable in the parasites after 72 h post infection. From that point on, both proteins were detected until the last time analyzed, 120 h after infection.

3.4. Changes occur in TcOGNT-2 RNA levels and in the 3′ UTR length along the life cycle

To further investigate the basis of the differential regulation of *Tc*OGNT-2 we explored its mRNA levels in epimastigotes, amastigotes and trypomastigotes by Real Time PCR. We found similar levels of *Tc*OGNT-2 mRNA in epimastigotes and trypomastigotes (Fig. 4A), however, *Tc*OGNT-2 mRNA levels decreased significantly (about 50%) in amastigotes at 24 h post infection when compared to those in the trypomastigote stage. In contrast, at 72 h post infection parasites showed the highest levels of *Tc*OGNT-2 expression suggesting that there is expression regulation of this gene upon amastigote differentiation and/or in the course of the infection process. Taking into account that the 3′ UTR of mRNAs are known to be involved in

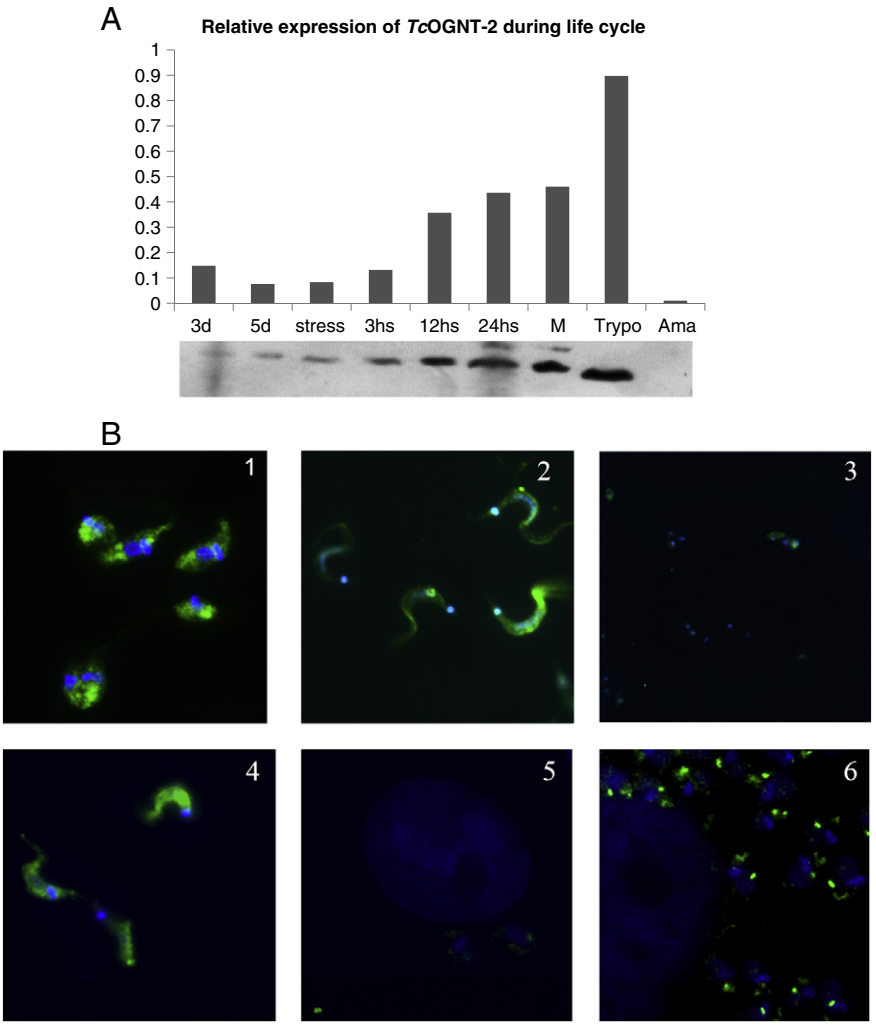

Fig. 2. Expression of *Tc*OGNT-2 during the life cycle of *T. cruzi*.A. Relative expression of *Tc*OGNT-2 during metacyclogenesis, cell-derived trypomastigotes and amastigotes: the expression of *Tc*OGNT-2 was estimated by densitometry using the GBox from Syngene with the GeneSnap and GeneTool softwares. The intensity of *Tc*OGNT-2 in western blot was compared with c*Tc*TXNPx expression, and the ratio *Tc*OGNT-2/c*Tc*TXNPx is represented in the graphic. 50 μg of protein extract during TAU metacyclogenesis, cell derived trypomastigotes and amastigotes: Lane 1: 3 day epimastigotes, 2: 5 day epimastigotes, 3: stress, 4: 3 h post stress, 5: 12 h, 6: 24 h, 7: metacyclic trypomastigotes, 8: cell derived trypomastigotes and 9: amastigotes were probed with anti *Tc*OGNT-2 antisera or antisera against c*Tc*TXNPx.B: Indirect immunofluorescence of epimastigotes (1), metacyclic trypomastigotes (2), axenic amastigotes (3), trypomastigotes (4), intracellular amastigotes at 24 h post infection (5), intracellular amastigotes at 72 h post infection (6), stained with DAPI and labeled with anti-*Tc*OGNT-2 purified antibody.

regulation of gene expression in *T. cruzi* (D'Orso et al., 2003; Jager et al., 2008; Nozaki and Cross, 1995), we also studied the length of these regions in mRNAs isolated from each stage. As shown in Fig. 4B, the amplification and sequencing of the 3′ UTRs revealed length differences between the three analyzed stages of the parasite, the shortest 3′ UTR being that from the amastigote stage. To ascertain if these differences can explain differences in mRNA stability further studies need to be conducted. It should be noted here that no differences were found in the 5′-UTR from the different stages (data not shown).

Interestingly, the analysis of the upstream genomic region where *Tc*OGNT-2 is located (chromosome 17), revealed the presence of four contiguous *trans*-sialidase genes (Supplementary Figure S1).

3.5. Overexpression of TcOGNT-2 enhances T. cruzi infectivity

There is evidence supporting the hypothesis that *O*-glycans and sialoglycans are involved in parasite–host cell adhesion and invasion (Acosta-Serrano et al., 2001; Neira et al., 2003; Turner et al., 2002; Yoshida et al., 1997), protection against proteases as well as immuno modulation (Alcaide and Fresno, 2004). To investigate the role of *Tc*OGNT-2 during the infection process, *T. cruzi* parasites overexpressing the gene were obtained.

The coding region of *Tc*OGNT-2 was inserted into the pTEX vector (Kelly et al., 1992) and the generated construct pTEX-TcOGNT-2 was used to transfect *T. cruzi* epimastigotes. Overexpression was confirmed by both, real time PCR and Western blot. mRNA levels increased threefold (data not shown) and Western blot analysis showed that *Tc*OGNT-2 protein is overexpressed more than six times in the transfected parasites (Fig. 5A). No differences were found in the growth rates of the transfectants when compared either to pTEX transfected or wild type parasites (data not shown).

In order to study the role of *Tc*OGNT-2 in mammalian host cell infection, we evaluated whether there were differences in the invasion and infection capability of overexpressing parasites when compared to controls. Invasion capacity was evaluated by counting the number of infected Vero cells and the number of intracellular parasites after 4 h of interaction. No differences were observed in the invasion capacity of *Tc*OGNT-2 overexpressing parasites in comparison with controls (Fig. 5B). However, infectivity, evaluated as the number of amastigotes per infected cell at 72 h post infection, proved to be 30% higher in parasites overexpressing *Tc*OGNT-2 (Fig. 5B).

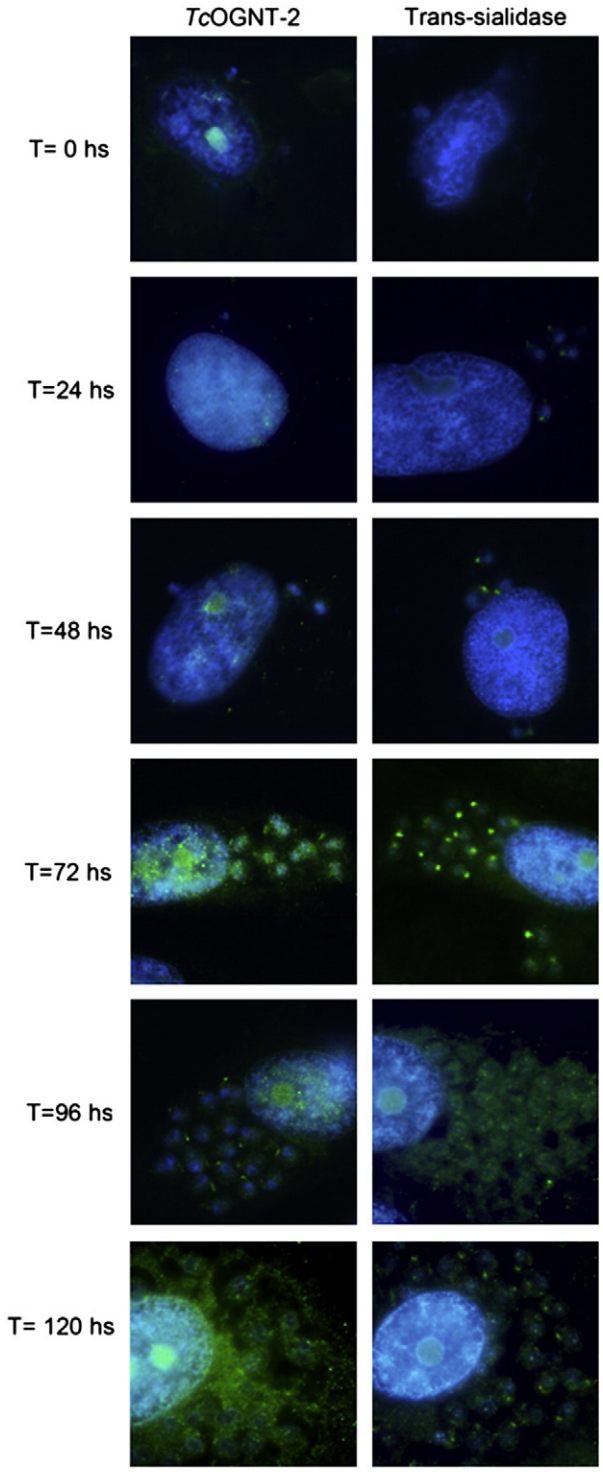

Fig. 3. Co-expression of *Tc*OGNT-2 and TS during an Infection of Vero Cells.Inmunofluorescence of Vero cells infected with trypomastigotes, the coverslips were removed and fixed at different times post infection and stained with DAPI for visualization of nucleus and kinetoplast. For *Tc*OGNT-2 and *trans*-sialidase visualization, anti-*Tc*OGNT-2 (1:200) polyclonal antibody or monoclonal antibody anti TS were used. Alexa 488 conjugated anti rabbit or anti mouse (1:500) was used as secondary antibodies respectively.

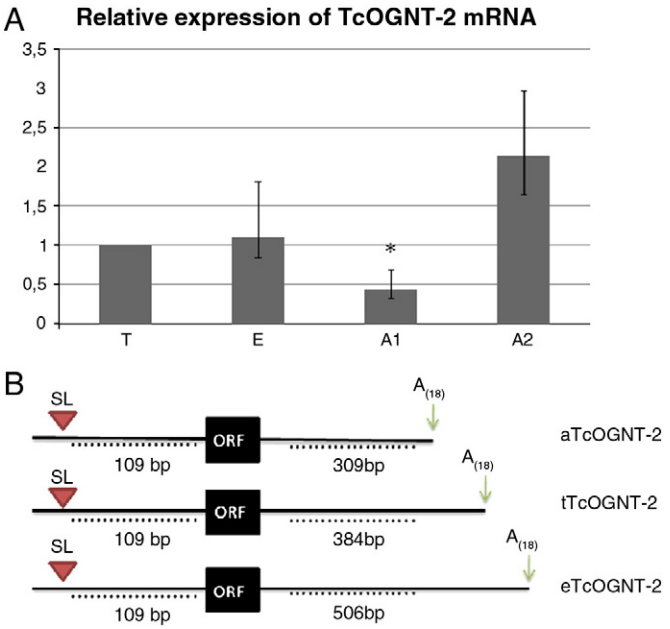

Fig. 4. mRNA expression and analysis of UTR region.A: *Tc*OGNT-2 mRNA levels were compared at different stages by real time PCR using specific primers for *Tc*OGNT-2. E (epimastigotes), T (trypomastigotes), A1 (amastigotes 24 h post infection) and A2 (amastigotes 72 h post infection). The results were analyzed with the ΔΔCt method and samples were normalized to GAPDH gene and compared against trypomastigotes RNA amount. Asterisk (*) represents significantly different from trypomastigotes, $p<0.05$. B: Schematic drawing (not to scale) representing 5′ and 3′ UTR regions of trypomastigotes, epimastigotes and amastigotes from Dm28c strain. The spliced leader addition site is indicated as SL; ORF indicates the open reading frame encoding *Tc*OGNT-2.

4. Discussion

The surface of the *T. cruzi* parasite is covered by mucins, mucin-like glycoproteins and *trans*-sialidases, which participate in adhesion, parasite protection, immune response modulation, establishment and persistence of infection. The relevance of these surface proteins is evidenced through the high representation of its genes in the parasite's genome, where approximately 50% of the coding regions encode these surface molecules (Epting et al., 2010).

In most eukaryotic organisms initiation of mucin like *O*-glycosylation implies the transfer of a GalNAc residue from UDP-GalNAc to Ser/Thr residues, a reaction which is catalyzed by a large family of evolutionarily conserved enzymes, the UDP-GalNAc:polypeptide-N-Acetylgalactosaminyltransferases (ppGalNAcTs), and it constitutes the limiting step in mucin maturation. A remarkable

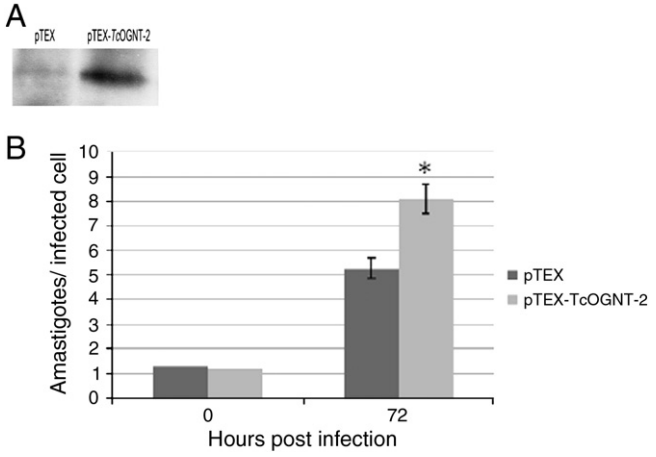

Fig. 5. *Tc*OGNT-2 over expression.A: Western blot with 30 μg of total extract proteins of epimastigotes transfected with pTEX or pTEX-*Tc*OGNT-2. The membranes were incubated with anti *Tc*OGNT-2 antibody. B: Infection assays with Vero cells and control trypomastigotes or overexpressing *Tc*OGNT-2. The number of amastigotes per infected cell was determined at 0 and 72 h post infection in 100 cells. Results are expressed as mean value ± SD of two independent experiments. Asterisks (*) represent significant differences between pTEX and over expressing parasites.

difference that occurs in *T. cruzi* with respect to mammals is the fact that this first limiting step in mucin-type *O*-glycosylation is catalyzed by a UDP-GlcNAc:polypeptide-N-Acetylgalactosaminyltransferase (ppGlcNAc-T) activity (Previato et al., 1998). The recent characterization of the ppGlcNAc-T coding gene in *T. cruzi* (*Tc*OGNT-2) led us to further characterization of this gene.

As ppGalNAc-Transferases (Ten Hagen et al., 2003), *Tc*OGNT-2 is also predicted to be located in the Golgi apparatus: structural analyses predict a type II transmembrane protein located in the lumen of this organelle. This fact is supported by evidence indicating that GlcNAc transferase activity is present in the Golgi apparatus (Morgado-Diaz et al., 2001; Previato et al., 1998). When subcellular fractions were analyzed by Western blot we found enrichment of *Tc*OGNT-2 in the microsomal fraction (that comprises the Golgi apparatus and Golgi-derived vesicles) as we expected. In order to confirm its localization we performed IIF with a Golgi marker, finding that *Tc*OGNT-2 is located in the Golgi apparatus, and surprisingly we observed that the protein is also present in reservosomes. The same pattern of distribution was found by electron microscopy (data not shown). Reservosomes have been described to be located in the posterior region of the epimastigote form of the parasite (de Souza et al., 2000) and one of their functions is the storage of lipids and proteins, although the complexity of their internal structure might reflect other multiple functions (Sant'Anna et al., 2008b). These organelles result from the fusion of vesicles originating in the plasma membrane during the endocytic pathway with vesicles trafficking from the endoplasmic reticulum–Golgi complex via the secretory pathway. We observed that ceramide, a Golgi complex marker, appeared with a dotted distribution mainly next to the kinetoplast, where the Golgi complex and the flagellar pocket are situated; but it was also faintly distributed in the posterior region of the parasite. This might be explained by the trafficking of proteins and lipids between the Golgi apparatus and the reservosomes where they are stored (Sant'Anna et al., 2009). Although reservosomes have been described in epimastigotes, all the stages of *T. cruzi* present reservosome-like organelles (Sant'Anna et al., 2008b). Nevertheless, their localization in trypomastigotes is in round compartments localized between nucleus and kinetoplast (Sant'Anna et al., 2008b), with a similar localization as the Golgi complex, in coincidence with our observation (Fig. 2B). In spite of this finding, the role of *Tc*OGNT-2 in reservosomes remains unclear. Interestingly, our results are reinforced by a recently published proteomic characterization of reservosomes (Sant'Anna et al., 2009) where this protein and another UDP-GlcNAc transferase-like protein (Acc. Number XP_814599) were detected, suggesting a more general role for *O*-glycosylation in these organelles.

This study reveals that *Tc*OGNT-2 shows a notorious differential expression along the life cycle of *T. cruzi*, which is almost completely undetectable in the replicative and intracellular amastigote stages. Moreover, when trypomastigotes penetrate Vero cells and differentiate into amastigotes, *Tc*OGNT-2 expression declines drastically at 48 h post infection. However, at 96 h, when intracellular amastigotes start to differentiate into trypomastigotes, the *Tc*OGNT-2 expression increases again. Interestingly, both mucin like proteins and *trans*-sialidases are also developmentally regulated in *T. cruzi*. It has been demonstrated that members of the *Tc*MUC I family are preferentially expressed in the amastigote stage while those of *Tc*MUCII are down regulated in amastigotes and overexpressed in trypomastigotes (Buscaglia et al., 2006; Minning et al., 2009) leading us to propose that members of the *Tc*MUCII family constitute substrates for *Tc*OGNT-2, which should imply a functional coordination with trypomastigote specific *trans*-sialidases (TS and TS I, see below). The function of *trans*-sialidases is essential, since *T. cruzi* parasites are unable to synthesize sialic acid *de novo*, they have gained the fascinating ability to acquire it from the host cell. The *trans*-sialidase family has been classified into three groups, two of them (TS and TS I) being expressed in both metacyclic and cell derived trypomastigotes. The common feature of these groups is the presence of a C-terminal extension with repeats of 12 amino acids named SAPA repeats (Frasch, 2000). It should be noted that the initial incorporation of GlcNAc through ppGlcNAc-T is a limiting and essential step for the trans-sialidation reaction, so we can speculate that both actions must be coordinated. In this sense, we compared the expression of both proteins during the intracellular infection, including early, medium and late infection, by using an anti-SAPA antibody, in order to detect only TS and TS I expression. We found that both enzymes are switched off during the early infection process, however, when amastigotes start the differentiation to trypomastigotes, evidenced by the presence of intracellular slender forms with higher motility, both enzymes begin to be expressed again. These results support the hypothesis of a co-expression of both enzymes, that are functionally related, and allow us to hypothesize that there is a functional relationship between the expression of *Tc*MUC II and the co-expression of *Tc*OCNT-2 and TS in trypomastigotes, although further experiments are necessary in order to demonstrate it.

A correspondence between differential expression at the protein and mRNA levels was evidenced by comparing western blot analysis and real time PCR: low levels of *Tc*OGNT-2 mRNA and protein were found in amastigotes. This result, although usual in higher eukaryotes, contrasts with that observed for several genes of trypanosomatids, in which gene expression regulation operates mainly at the post-transcriptional level, and therefore needs further analysis. In these parasites, different levels of mRNA mostly reflect differences in stability, and the 3′ untranslated regions of many parasite genes have been involved in this mRNA stability regulation (Clayton and Shapira, 2007; Nozaki and Cross, 1995).

Interestingly, it was previously reported that the 3′ UTR of *trans*-sialidase is directly involved in the stage specific expression of this enzyme. In this work we analyzed the 3′ UTR of *Tc*OGNT-2 mRNAs from amastigotes, epimastigotes and trypomastigotes through RT-PCR, using a specific forward primer and an oligo-dT primer with an anchor sequence, and we found that the 3′ UTR from amastigotes was shorter than those from trypomastigotes and epimastigotes. We postulate that this shorter 3′ UTR can directly affect the stability of the mRNA in the amastigote stage, causing a decrease in *Tc*OGNT-2 expression. However, further studies with reporter genes are needed in order to demonstrate the relevance of this mechanism. Finally we cannot discard a transcriptional regulation due to the proximity of *Tc*OGNT-2 and TS genes in the genome (Supplementary Fig. 1).

Considering that *Tc*OGNT-2 participates in the first step of *O*-glycosylation, and taking into account that mucins play a relevant role in *T. cruzi* virulence and infectivity (Yoshida, 2006), we investigated whether the overexpression of *Tc*OGNT-2 could have some effect on the infectivity of these parasites. We found that parasites overexpressing *Tc*OGNT-2 are more infective than controls. This finding could be explained by the fact that *Tc*OGNT-2 overexpression results in surface alterations where molecules involved in the infection process may be affected. Particularly, the participation of *Tc*OGNT-2 in the first step of *O*-glycosylation, which is necessary for further incorporation of galactoses and finally sialic acid to mucins, may be directly related with the observed higher infectivity. Altogether these results lead us to propose new experiments in order to evaluate this enzyme as a possible target for drug design.

Supplementary materials related to this article can be found online at doi:10.1016/j.gene.2012.02.018.

Acknowledgments

We thank Dr. Oscar Campetella and J.J. Cazzulo (Instituto de Investigaciones Biotecnológicas, Universidad Nacional de San Martín) for kindly providing anti-SAPA and anti-cruzipain antibodies respectively; Monica Gardner (Institut Pasteur de Montevideo) for revision of the manuscript; and Paula Faral and Lorena Gil (Institut Pasteur de Montevideo) for technical assistance.

This work was supported by grants from the "Agencia Nacional de Investigación e Innovación" ANII (FCE2007_357) and a research fellowship

from the ANII (MLC). A.P.T., E.O. and C.R. are researchers from the Sistema Nacional de Investigadores (ANII), Montevideo, Uruguay.

References

Acosta, A., Schenkman, R.P., Schenkman, S., 1994. Sialic acid acceptors of different stages of *Trypanosoma cruzi* are mucin-like glycoproteins linked to the parasite membrane by GPI anchors. Braz. J. Med. Biol. Res. 27, 439–442.

Acosta-Serrano, A., Almeida, I.C., Freitas-Junior, L.H., Yoshida, N., Schenkman, S., 2001. The mucin-like glycoprotein super-family of *Trypanosoma cruzi*: structure and biological roles. Mol. Biochem. Parasitol. 114, 143–150.

Alcaide, P., Fresno, M., 2004. The *Trypanosoma cruzi* membrane mucin AgC10 inhibits T cell activation and IL-2 transcription through L-selectin. Int. Immunol. 16, 1365–1375.

Almeida, I.C., Ferguson, M.A., Schenkman, S., Travassos, L.R., 1994. Lytic anti-alpha-galactosyl antibodies from patients with chronic Chagas' disease recognize novel O-linked oligosaccharides on mucin-like glycosyl-phosphatidylinositol-anchored glycoproteins of *Trypanosoma cruzi*. Biochem. J. 304 (Pt 3), 793–802.

Almeida, I.C., et al., 2000. Highly purified glycosylphosphatidylinositols from *Trypanosoma cruzi* are potent proinflammatory agents. EMBO J. 19, 1476–1485.

Araguth, M.F., Rodrigues, M.M., Yoshida, N., 1988. *Trypanosoma cruzi* metacyclic trypomastigotes: neutralization by the stage-specific monoclonal antibody 1G7 and immunogenicity of 90 kD surface antigen. Parasite Immunol. 10, 707–712.

Atwood III, J.A., et al., 2005. The *Trypanosoma cruzi* proteome. Science 309, 473–476.

Buscaglia, C.A., Campetella, O., Leguizamon, M.S., Frasch, A.C., 1998. The repetitive domain of *Trypanosoma cruzi* trans-sialidase enhances the immune response against the catalytic domain. J. Infect. Dis. 177, 431–436.

Buscaglia, C.A., Campo, V.A., Frasch, A.C., Di Noia, J.M., 2006. *Trypanosoma cruzi* surface mucins: host-dependent coat diversity. Nat. Rev. Microbiol. 4, 229–236.

Chuenkova, M., Pereira, M.E., 1995. *Trypanosoma cruzi* trans-sialidase: enhancement of virulence in a murine model of Chagas' disease. J. Exp. Med. 181, 1693–1703.

Clayton, C., Shapira, M., 2007. Post-transcriptional regulation of gene expression in trypanosomes and leishmanias. Mol. Biochem. Parasitol. 156, 93–101.

Contreras, V.T., Salles, J.M., Thomas, N., Morel, C.M., Goldenberg, S., 1985. In vitro differentiation of *Trypanosoma cruzi* under chemically defined conditions. Mol. Biochem. Parasitol. 16, 315–327.

Cunha-e-Silva, N., Sant'Anna, C., Pereira, M.G., Porto-Carreiro, I., Jeovanio, A.L., de Souza, W., 2006. Reservosomes: multipurpose organelles? Parasitol. Res. 99, 325–327.

de Lederkremer, R.M., Agusti, R., 2009. Glycobiology of *Trypanosoma cruzi*. Adv. Carbohydr. Chem. Biochem. 62, 311–366.

de Souza, W., Carreiro, I.P., Miranda, K., Silva, N.L., 2000. Two special organelles found in *Trypanosoma cruzi*. An. Acad. Bras. Cienc. 72, 421–432.

Di Noia, J.M., D'Orso, I., Aslund, L., Sanchez, D.O., Frasch, A.C., 1998. The *Trypanosoma cruzi* mucin family is transcribed from hundreds of genes having hypervariable regions. J. Biol. Chem. 273, 10843–10850.

D'Orso, I., De Gaudenzi, J.G., Frasch, A.C., 2003. RNA-binding proteins and mRNA turnover in trypanosomes. Trends Parasitol. 19, 151–155.

El-Sayed, N.M., et al., 2005. The genome sequence of *Trypanosoma cruzi*, etiologic agent of Chagas disease. Science 309, 409–415.

Epting, C.L., Coates, B.M., Engman, D.M., 2010. Molecular mechanisms of host cell invasion by *Trypanosoma cruzi*. Exp. Parasitol. 126, 283–291.

Frasch, A.C., 2000. Functional diversity in the trans-sialidase and mucin families in *Trypanosoma cruzi*. Parasitol. Today 16, 282–286.

Freire-de-Lima, L., et al., 2010. *Trypanosoma cruzi* subverts host cell sialylation and may compromise antigen-specific CD8 + T cell responses. J. Biol. Chem. 285, 13388–13396.

Freitas-Junior, L.H., Briones, M.R., Schenkman, S., 1998. Two distinct groups of mucin-like genes are differentially expressed in the developmental stages of *Trypanosoma cruzi*. Mol. Biochem. Parasitol. 93, 101–114.

Frevert, U., Schenkman, S., Nussenzweig, V., 1992. Stage-specific expression and intracellular shedding of the cell surface trans-sialidase of *Trypanosoma cruzi*. Infect. Immun. 60, 2349–2360.

Heise, N., et al., 2009. Molecular analysis of a UDP-GlcNAc:polypeptide alpha-N-acetylglucosaminyltransferase implicated in the initiation of mucin-type O-glycosylation in *Trypanosoma cruzi*. Glycobiology 19, 918–933.

Jager, A.V., Muia, R.P., Campetella, O., 2008. Stage-specific expression of *Trypanosoma cruzi* trans-sialidase involves highly conserved 3′ untranslated regions. FEMS Microbiol. Lett. 283, 182–188.

Jensen, P.H., Kolarich, D., Packer, N.H., 2010. Mucin-type O-glycosylation—putting the pieces together. FEBS J. 277, 81–94.

Kelly, J.M., Ward, H.M., Miles, M.A., Kendall, G., 1992. A shuttle vector which facilitates the expression of transfected genes in *Trypanosoma cruzi* and *Leishmania*. Nucleic Acids Res. 20, 3963–3969.

Minning, T.A., Weatherly, D.B., Atwood III, J., Orlando, R., Tarleton, R.L., 2009. The steady-state transcriptome of the four major life-cycle stages of *Trypanosoma cruzi*. BMC Genomics 10, 370.

Morgado-Diaz, J.A., et al., 2001. Isolation and characterization of the Golgi complex of the protozoan *Trypanosoma cruzi*. Parasitology 123, 33–43.

Mortara, R.A., da Silva, S., Araguth, M.F., Blanco, S.A., Yoshida, N., 1992. Polymorphism of the 35- and 50-kilodalton surface glycoconjugates of *Trypanosoma cruzi* metacyclic trypomastigotes. Infect. Immun. 60, 4673–4678.

Mucci, J., Hidalgo, A., Mocetti, E., Argibay, P.F., Leguizamon, M.S., Campetella, O., 2002. Thymocyte depletion in *Trypanosoma cruzi* infection is mediated by trans-sialidase-induced apoptosis on nurse cells complex. Proc. Natl. Acad. Sci. U. S. A. 99, 3896–3901.

Neira, I., Silva, F.A., Cortez, M., Yoshida, N., 2003. Involvement of *Trypanosoma cruzi* metacyclic trypomastigote surface molecule gp82 in adhesion to gastric mucin and invasion of epithelial cells. Infect. Immun. 71, 557–561.

Nozaki, T., Cross, G.A., 1995. Effects of 3′ untranslated and intergenic regions on gene expression in *Trypanosoma cruzi*. Mol. Biochem. Parasitol. 75, 55–67.

Pereira-Chioccola, V.L., et al., 2000. Mucin-like molecules form a negatively charged coat that protects *Trypanosoma cruzi* trypomastigotes from killing by human anti-alpha-galactosyl antibodies. J. Cell Sci. 113 (Pt 7), 1299–1307.

Previato, J.O., Andrade, A.F., Pessolani, M.C., Mendonca-Previato, L., 1985. Incorporation of sialic acid into *Trypanosoma cruzi* macromolecules. A proposal for a new metabolic route. Mol. Biochem. Parasitol. 16, 85–96.

Previato, J.O., et al., 1998. Biosynthesis of O-N-acetylglucosamine-linked glycans in *Trypanosoma cruzi*. Characterization of the novel uridine diphospho-N-acetylglucosamine:polypeptide N-acetylglucosaminyltransferase-catalyzing formation of N-acetylglucosamine alpha1→O-threonin. J. Biol. Chem. 273, 14982–14988.

Roper, J.R., Ferguson, M.A., 2003. Cloning and characterisation of the UDP-glucose 4′-epimerase of *Trypanosoma cruzi*. Mol. Biochem. Parasitol. 132, 47–53.

Ruiz Rde, C., Rigoni, V.L., Gonzalez, J., Yoshida, N., 1993. The 35/50 kDa surface antigen of *Trypanosoma cruzi* metacyclic trypomastigotes, an adhesion molecule involved in host cell invasion. Parasite Immunol. 15, 121–125.

Sambrook, J., Maniatis, T., Fritsch, E.F., 1989. Molecular Cloning: a Laboratory Manual. Cold Spring Harbor Laboratory, Cold Spring Harbor, N.Y.

Sant'Anna, C., Parussini, F., Lourenco, D., de Souza, W., Cazzulo, J.J., Cunha-e-Silva, N.L., 2008a. All *Trypanosoma cruzi* developmental forms present lysosome-related organelles. Histochem. Cell Biol. 130, 1187–1198.

Sant'Anna, C., Pereira, M.G., Lemgruber, L., de Souza, W., Cunha e Silva, N.L., 2008b. New insights into the morphology of *Trypanosoma cruzi* reservosome. Microsc. Res. Tech. 71, 599–605.

Sant'Anna, C., et al., 2009. Subcellular proteomics of *Trypanosoma cruzi* reservosomes. Proteomics 9, 1782–1794.

Ten Hagen, K.G., Fritz, T.A., Tabak, L.A., 2003. All in the family: the UDP-GalNAc:polypeptide N-acetylgalactosaminyltransferases. Glycobiology 13, 1R–16R.

Tribulatti, M.V., Mucci, J., Van Rooijen, N., Leguizamon, M.S., Campetella, O., 2005. The trans-sialidase from *Trypanosoma cruzi* induces thrombocytopenia during acute Chagas' disease by reducing the platelet sialic acid contents. Infect. Immun. 73, 201–207.

Turner, C.W., Lima, M.F., Villalta, F., 2002. *Trypanosoma cruzi* uses a 45-kDa mucin for adhesion to mammalian cells. Biochem. Biophys. Res. Commun. 290, 29–34.

Yoshida, N., 2006. Molecular basis of mammalian cell invasion by *Trypanosoma cruzi*. An. Acad. Bras. Cienc. 78, 87–111.

Yoshida, N., Mortara, R.A., Araguth, M.F., Gonzalez, J.C., Russo, M., 1989. Metacyclic neutralizing effect of monoclonal antibody 10D8 directed to the 35- and 50-kilodalton surface glycoconjugates of *Trypanosoma cruzi*. Infect. Immun. 57, 1663–1667.

Yoshida, N., Blanco, S.A., Araguth, M.F., Russo, M., Gonzalez, J., 1990. The stage-specific 90-kilodalton surface antigen of metacyclic trypomastigotes of *Trypanosoma cruzi*. Mol. Biochem. Parasitol. 39, 39–46.

Yoshida, N., Dorta, M.L., Ferreira, A.T., Oshiro, M.E., Mortara, R.A., Acosta-Serrano, A., Favoreto Junior, S., 1997. Removal of sialic acid from mucin-like surface molecules of *Trypanosoma cruzi* metacyclic trypomastigotes enhances parasite–host cell interaction. Mol. Biochem. Parasitol. 84, 57–67.